Zeitschrift: IABSE proceedings = Mémoires AIPC = IVBH Abhandlungen
Band: 14 (1990)
Heft: P-143: Analysis of the elastic response of stay and stayed systems

Artikel: Analysis of the elastic response of stay and stayed systems
Autor: Bruno, Domenico / Maceri, Franco / Olivito, Renato S.
DOI: https://doi.org/10.5169/seals-42835

Analysis of the Elastic Response of Stay and Stayed Systems

Etude du comportement élastique de haubans et de systèmes haubanés

Analyse des elastischen Verhaltens von Abspannungen und Abspannsystemen

Domenico BRUNO
Assoc. Professor
University of Calabria
Cosenza, Italy

Domenico Bruno, born 1949, received his civil engineering degree at the University of Naples, Italy. Associate Professor of Structural Engineering at the Dep. of Structures, University of Calabria, presently carrying out research on mechanics of composite structures and problems in structural mechanics.

Franco MACERI
Professor
Univ. of Rome «Tor Vergata»
Rome, Italy

Franco Maceri, born 1941, received his engineering «laurea» in 1963 at University of Naples, Italy. From 1976 to 1982, he was professor of Theory of Structures and Dean of Engineering at University of Calabria. Presently, he is Full Professor of Structural Engineering and President of Civil Engineering Courses at University of Rome «Tor Vergata». Professor Maceri's main fields of interest are: computerized structural analysis, problems in structural mechanics, large structures.

Renato S. OLIVITO
Assoc. Professor
University of Calabria
Cosenza, Italy

Renato S. Olivito, born 1950, received his engineering degree at the Polytechnic of Turin, Italy. Presently he is Associate Professor of Structural Engineering at the Dep. of Structures, Univ. of Calabria. His field of research mainly concerns experimental mechanics of materials and civil engineering structures. Other topics of research include experimental analysis of long-span cable-stayed bridges, contact problems and no-tension materials like masonry structures.

SUMMARY

This paper investigates the static behaviour of elastic stays and stayed systems under dead load and axial thrust. A theoretical analysis is proposed using a finite element approach which accounts for the geometrical non-linear effects. An experimental investigation confirmed the soundness of the numerical results previously obtained.

RÉSUMÉ

Cet article étudie le comportement statique de haubans élastiques et de systèmes haubanés sous l'effet du poids propre et d'un effort normal. Une analyse théorique est réalisée à l'aide d'une méthode par éléments finis qui tient compte de l'état géométrique non-linéaire. L'exactitude des résultats numériques est confirmée par des essais.

ZUSAMMENFASSUNG

In dieser Arbeit wird das statische Verhalten von elastischen Abspannungen und Abspannsystemen unter Eigenlast und Normalkraft untersucht. Eine theoretische Analyse mit Hilfe der Methode der finiten Elemente wird vorgeschlagen, die nichtlineare Effekte zu berücksichtigen gestattet. Eine experimentelle Untersuchung bestätigt die berechneten Resultate.

1. INTRODUCTION.

The statical behaviour of elastic cables is a widely investigated problem. In recent years, a number of new studies appeared, owing to the growing structural use of cable systems, especially networks and trusses.

In particular, we are interested in the use of cables as stays or counter-stayed elements in cable-stayed bridges. Therefore, the elastic response of such elements to an increment of axial thrust will be primarily investigated.

Dischinger's fictitious moduli theory is well known. However, this approach applies when the initial axial stress is sufficiently high. Therefore, we first briefly recall the exact formulation of the elastic equilibrium of a single stay subject to a constant dead load and to an axial thrust, then we provide finite element computation schemes useful for the analysis of stays and stayed systems, at least for the case of largely bent initial configurations. By these methods we provide a validation of the basic Dischinger theory and we give an estimation of the inherent error at low stress levels.

Further, we study the elastic response of a counterstayed stay.

The results of experimental investigations are then given, which point out a good agreement with the nonlinear theory, implemented via finite elements, and, in the case of high initial stress, with Dischinger's approximate analysis.

2. THE ELASTIC CABLE: THEORETICAL PRELIMINARIES.

Let us consider a cable C fixed at its end S_1 and subject at S_2 (fig. 1) to a thrust F through S_1, S_2, and denote by T the horizontal component of cable tension. The cable has no flexural stiffness, has a cross-sectional area A, and γ is its specific weight.

The equation of the elastic catenary, describing the cable's equilibrium configuration, is given by:

$$\frac{y}{L} = \frac{1}{\tau}\left[\cosh \tau \frac{x}{L} - 1\right] \quad , \tag{1}$$

where the dimensionless cable weight versus cable stress ratio τ is given by:

$$\tau = \frac{\gamma A L}{T} \quad , \tag{2}$$

and L is the horizontal projection of the chord $S_1 S_2$ of length l.

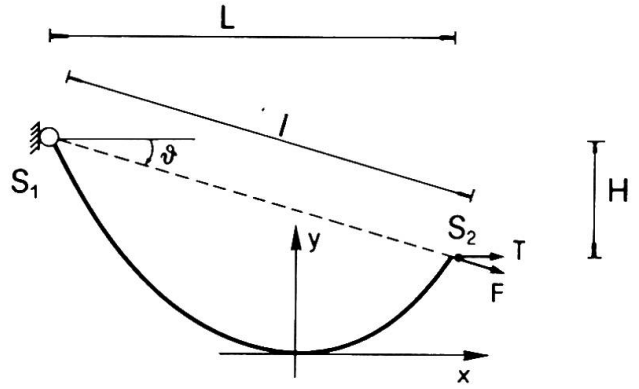

Fig. 1. The elastic cable: notation.

Let us denote by $\mathcal{L}$ the length of the elastic line in the deformed configuration, and by $\mathcal{L}_u$, $\Delta\mathcal{L}$ its unstressed length and the relative increment due to tensile stresses. We can write

$$\mathcal{L} = \mathcal{L}_u + \Delta\mathcal{L} \quad . \tag{3}$$

$\mathcal{L}$ and $\Delta\mathcal{L}$ values can be obtained by:

$$\mathcal{L} = \int_L \left(1 + y'^2\right)^{1/2} dx \quad , \quad \Delta\mathcal{L} = \frac{T}{EA}\int_L \left(1 + y'^2\right) dx \quad . \tag{4}$$

Let us now introduce the series development of the right-hand side of Eq. 1:

$$\frac{y}{L} = \frac{\tau}{2}\left[\frac{x}{L}\right]^2 + \frac{\tau^3}{4!}\left[\frac{x}{L}\right]^4 + \cdots \tag{5}$$

For high stress levels (i.e. $\tau \gg 1$), Eq. 5 can be replaced by its quadratic approximation, and in this case we obtain for Eq. 3 the approximate form (fig. 1):

$$l + \frac{\gamma^2 l^3}{24\sigma^2}\cos^2\theta = \mathcal{L}_u + \frac{\sigma l}{E} + \frac{\gamma^2 l^3}{12E\sigma}\cos^2\theta \quad , \tag{6}$$

where $\sigma = F/A$ is the dimensionless axial thrust.
To compute the elastic cable response, let us differentiate Eq. 6:

$$0 = d\mathcal{L}_u \implies \frac{d\sigma}{dl} = \frac{1 + (\gamma^2 l^2\cos^2\theta)/(8\sigma^2) - (\sigma/E) - (\gamma^2 l^2\cos^2\theta)/(4E\sigma)}{(\gamma^2 l^3\cos^2\theta)/(12\sigma^3) + (l/E) - (\gamma^2 l^2\cos^2\theta)/(12\sigma^2 E)} \quad . \tag{7}$$

Taking into account that $l\cdot\cos\theta = L$ and by introducing the apparent strain $\epsilon = dl/l$ we obtain from Eq. 7:

$$E_t^* = \frac{d\sigma}{dl}l = E\,\frac{1 + \tau^2/8 - (\sigma/E)\,(1+\tau^2/4)}{1 + (\gamma^2 L^2 E/12\sigma^3)(1 - (\sigma/E))} \simeq E\,\frac{1}{1 + \gamma^2 L^2 E/12\sigma^3} = E_{td}^* \quad . \tag{8}$$

In Eq. 8, E_{td}^* is the well-known Dischinger's tangent modulus formula.
To evaluate the inherent error in the quadratic approximation, we develop now the exact theory in the simple case of a cable with horizontal chord ($\theta = 0$). In this case Eq. 3, by putting $\omega = \sigma/E$, takes the form:

$$\frac{2}{\tau}\sinh\frac{\tau}{2} = \frac{\mathcal{L}_u}{L} + \frac{\omega}{2}\left[1 + \frac{1}{\tau}\sinh\tau\right] \quad . \tag{9}$$

Eq. 9 can be used in the following way. We assume that a cable is in equilibrium under its own (dimensionless) weight τ_0 and a (dimensionless) thrust ω_0: the unstressed length $\mathcal{L}_u$ in the reference configuration is then computed from Eq. 9. The parameter

$$\Lambda = \mathcal{L}_u/L \tag{10}$$

is then known, and Eq. 9 can be employed to derive, by simple computation, the $\tau - \omega$ interaction curves.

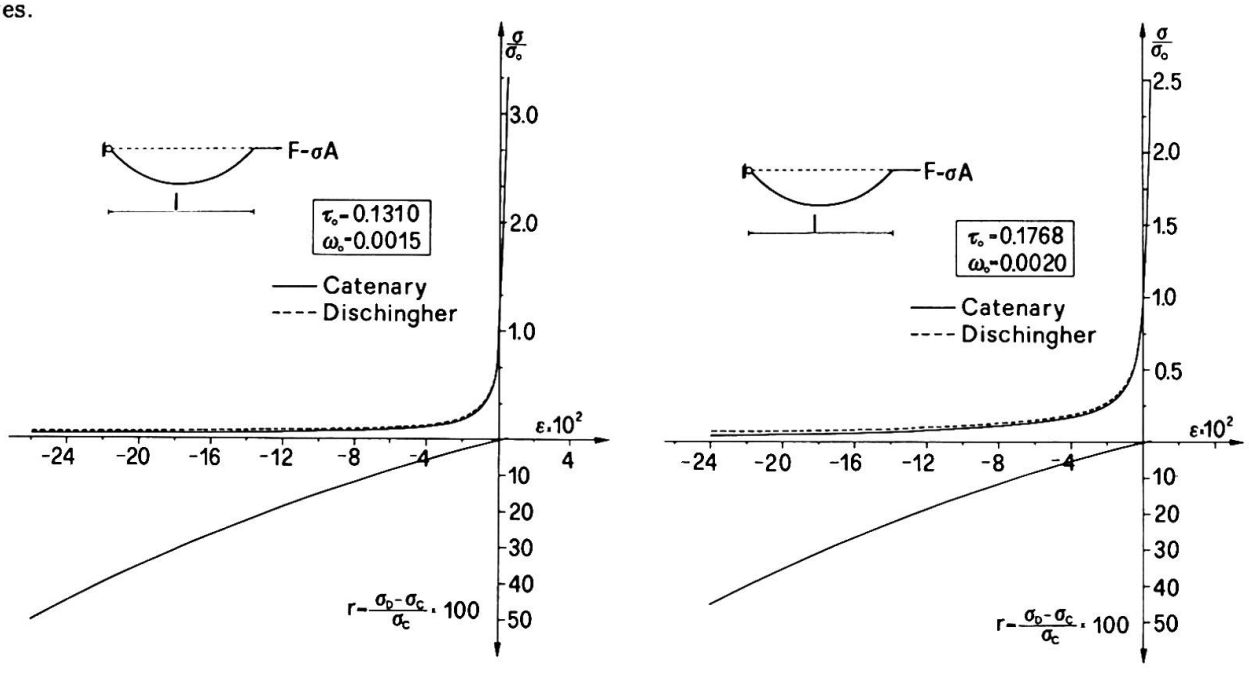

Fig. 2. Horizontal elastic cable. Comparison between catenary solution (σ_C) and Dischinger's approximate solution (σ_D) for different values of τ_0 and ω_0.

A numerical investigation was carried out with reference to τ_0, ω_0 values shown in fig. 2, corresponding to uniform steel cables ($E = 2.0075 \times 10^3\ t/cm^2$, $\sigma_0 = 3 \div 4\ t/cm^2$). In fig. 2.a, b, the exact solution obtained from Eq. 9 is compared with Dischinger's approximate results, obtained by integrating Eq. 8 along the $\sigma - \epsilon$ curve.
As is well known, this corresponds to assuming the following Dischinger's secant modulus E^*_{sd} value:

$$E^*_{sd} = \frac{E}{1 + (\gamma^2 L^2 E)(1+\beta)/24\sigma_0^3\beta^2} \tag{11}$$

between the initial stress σ_0 and the final one $\beta\sigma_0$.
From these results the soundness of Dischinger's theory is apparent in the case of high stress levels. On the contrary, when cable unloading to low stress levels occurs, as in the case of nonlinear stability analysis of cable-stayed bridges [14], to obtain accurate values, theories close to the catenary theory are needed.
A fortiori, such theories should be used to describe the behaviour of inclined stays and counter-stayed systems. In fact, in these cases, Dischinger's approach can give poor results, and the catenary theory, which is based on systems of nonlinear equations of the kind of Eq. 9, is very hard to solve.

3. NUMERICAL MODELS FOR STAY SYSTEMS ANALYSIS.

In this section, we describe two finite element models for the analysis of the nonlinear elastic behaviour of stays and stayed systems.

3.1 First model.

The first model is based on a nonlinear finite element model in which parabolic and cubic approximations for vertical and horizontal displacements v and u, respectively, are assumed (fig. 3).

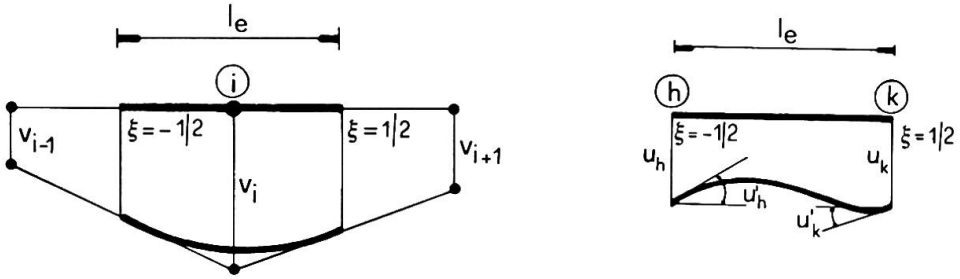

Fig. 3. First model: finite element scheme.

The following nonlinear strain measure is assumed:

$$\epsilon = \epsilon_0 + u_{,x} + \frac{1}{2} v_{,x}^2 \tag{12}$$

where ϵ_0 is the primitive strain in its initial reference configuration.
The elemental nodal force $\mathbf{s}_e$ and nodal load $\mathbf{p}_e$ vectors are obtained by means of the virtual work equation:

$$\int_{l_e} EA\epsilon\delta\epsilon\, dx - \int_{l_e^*} (p_x\delta u + p_y\delta v)\, ds = \delta\mathbf{d}_e^T(\mathbf{s}_e - \mathbf{p}_e) = 0\ ,\ \forall\delta\mathbf{d}_e \tag{13}$$

where $\mathbf{d}_e \equiv [\mathbf{u}_e\ ,\ \mathbf{v}_e]$ is the elemental nodal dispacement vector, the second integral is made on the deformed configuration of the stay's element and p_x, p_y are the dead load components per unit length of the deformed arch.
It should be noted that, by using this model, displacements u, v, their derivatives $u_{,x}$, $v_{,x}$ and strain ϵ are continuous along the complete stay.
Hence, the finite element discrete model converges to the continuous one.

3.2. Second model.

Let us assume that the stay element remain rectilinear in the deformed configuration (fig. 4) and that axial displacements are linear along the element.

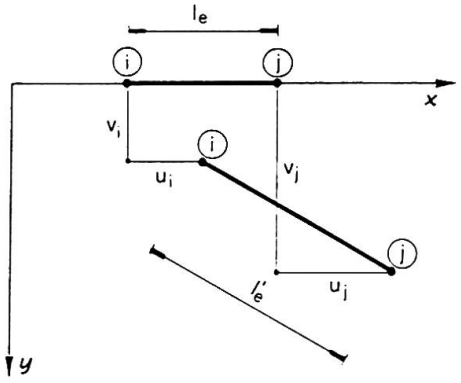

Fig. 4. Second model: finite element scheme.

Let us assume, further, that the stress state, constant within the element, is given by:

$$\sigma^e = \sigma_0^e + E_{sd}^*(\sigma^e)\Delta\epsilon^e \ , \tag{14}$$

where σ_0^e is the primitive stress in the initial reference configuration, $E_{sd}^*(\sigma^e)$ is the Dischinger secant modulus for the element, and

$$\Delta\epsilon^e = \frac{l'_e - l_e}{l_e} \ . \tag{15}$$

Then, the nodal force vector $\mathbf{s}_e$ is given by:

$$\mathbf{s}_e = \sigma^e A \mathbf{n}^e \ , \tag{16}$$

where $\mathbf{n}^e$ is the direction cosines vector of the element in the actual configuration.
This model can be justified by observing that the Dischinger formula's accuracy is very good for small values of l_e. Hence, the nonlinear effect may be entirely attributed to the geometry change. For this reason, the length variation of the element relative to the configuration change is exactly evaluated by using Eq. 15.
This second model offers the advantage of a smaller number of unknowns than the previous one, if the number of elements is the same.

3.3. Numerical procedure.

Both models previously formulated can be used, together with appropriate assembling techniques, to construct the complete structural model of a single stay or of a counter-stayed stay. In all cases, the nonlinear equilibrium equations, in terms of generalized nodal displacements as unknowns, have the form:

$$\mathbf{p}(\lambda) - \mathbf{s}(\mathbf{d}) = 0 \ , \tag{17}$$

where:
- $\mathbf{s}(\mathbf{d})$ is the generalized nodal forces vector,
- $\mathbf{p}(\lambda)$ is the generalized nodal loads vector.

We assume for $\mathbf{p}(\lambda)$ the following expression:

$$\mathbf{p}(\lambda) = \mathbf{p}_0 + \lambda \mathbf{p}_1 \ , \ \lambda \geq 0 \ , \tag{18}$$

where $\mathbf{p}_0$ is the load vector in the primitive configuration and $\lambda\mathbf{p}_1$ gives a linearly increasing contribution.
The nonlinear Eq. 17 is solved step–by–step, for discrete values λ_h of the load parameter λ . At each load step, the standard M. N. R. iterative scheme was used to solve the equilibrium equations.
This numerical procedure was used to find both the elastic response $\lambda - \mathbf{d}$ and the initial configuration Γ_0 corresponding to $\lambda = 0$.

3.4. Numerical results for single stay analysis.

We study the stay shown in fig. 5. It is well-known that the simplified Dischinger theory is based on the following assumption:

i) parabolic cable shape,

ii) constant tension along the cable.

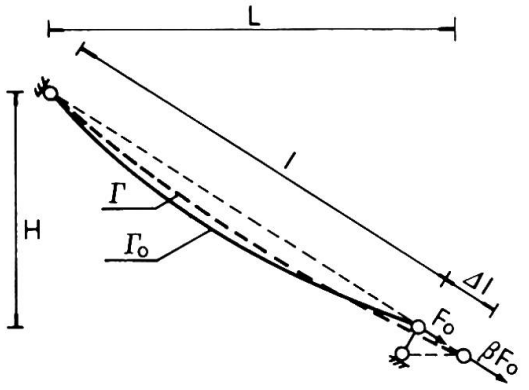

Fig. 5. Single stay scheme: notation.

The accuracy of Dischinger's formula (Eq. 11) has been investigated for different values of the characteristic parameters σ_0, L, β, by comparison with the numerical values of the secant modulus

$$E_s^* = \frac{\beta - 1}{\Delta l(\beta)} \frac{F_0 l}{A} \quad , \tag{19}$$

and of the tangent modulus

$$E_t^* = \lim_{\beta \to 1} E_s^* \quad , \tag{20}$$

obtained by using both models previously formulated.

The convergence of such models is first shown in tab. 1.

Table 1

L=1200 m **H=480 m** σ_0=**30000** t/m^2 **NE=Number of Elements**

	E_s^*/E					
	1st model			2nd model		
NE \ β	1.2	1.6	2.0	1.2	1.6	2.0
5	0.18952	0.26014	0.32250	0.18987	0.25987	0.32179
10	0.18940	0.26001	0.32237	0.19001	0.26001	0.32193
20	0.18936	0.25998	0.32234	0.19005	0.26005	0.32197
40	0.18936	0.25997	0.32233	0.19006	0.26006	0.32198
E_{sd}^*/E	0.18869	0.25918	0.32146	0.18869	0.25918	0.32146

In figs. 6.a, b, the influence of L on the elastic response curves $\sigma - \epsilon$ for two typical stays is shown. From these curves Eq.11 is shown to exhibit very good accuracy at high stress levels. On the other hand, significant discrepancies are present at low stress levels, in particular for longer spans.

Finally, in fig. 7, good agreement is shown between the secant modulus curves, evaluated according to Eq. 11, and the numerical nonlinear finite element results.

We conclude this section by observing that, according to these results, the second F.E. model can be validated.

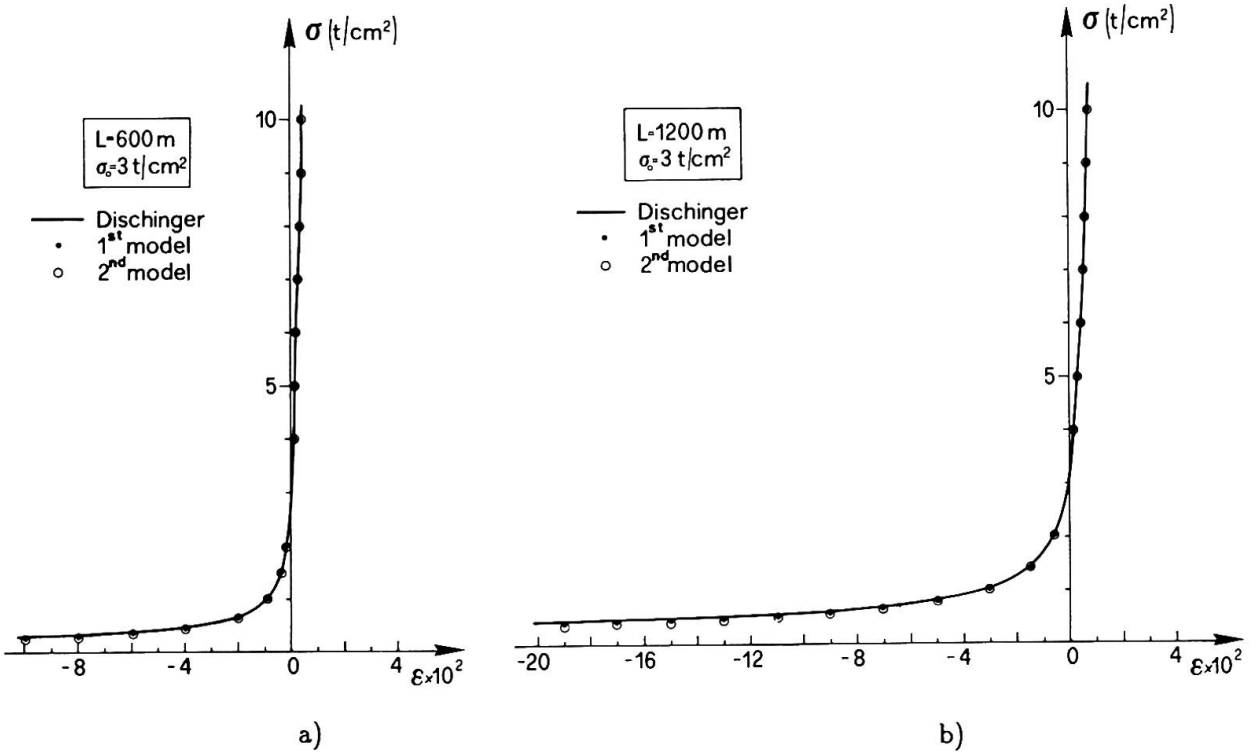

a) b)

Fig. 6. Single stay elastic response: influence of L.

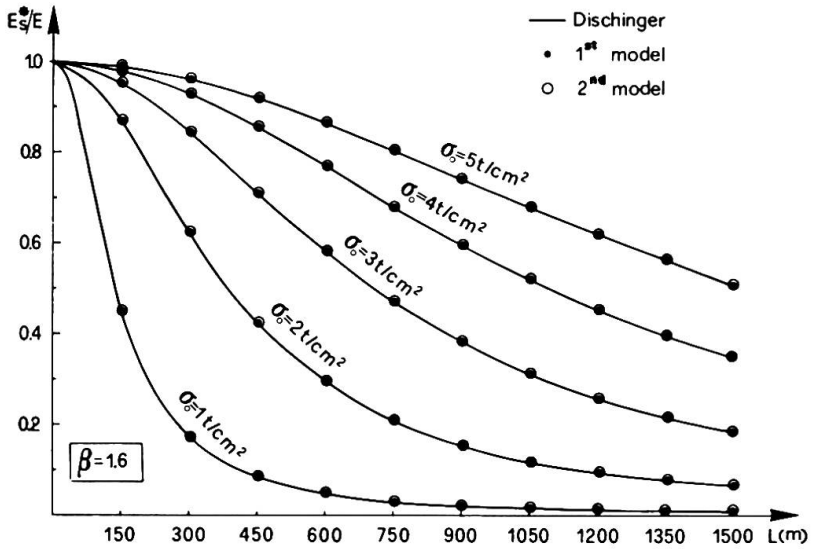

Fig. 7. Single stay elastic response: influence of σ_0.

4. COUNTER-STAYS EFFECT ANALYSIS.

In this section we analyze the stiffening effect due to a counter-stay system acting on a cable.

This feature, allowing a reduction of the loss of axial stiffness because of Dischinger's effect, is of primary importance to reduce also the overall bridge flexibility.

Thus, let us examine the scheme of fig. 8.

A first simplified analysis can be made adopting the usual Dischinger's assumption. In this case, we obtain the following expression for the secant modulus:

$$E_s^* = \frac{E_{sd}^{*(1)} \cdot E_{sd}^{*(2)}}{(1-\eta)E_{sd}^{*(1)} + \eta E_{sd}^{*(2)}} \quad , \tag{21}$$

where $E_{sd}^{*(1)}$, $E_{sd}^{*(2)}$ are, respectively, the Dischinger's secant moduli of stay's segments AB, BC.

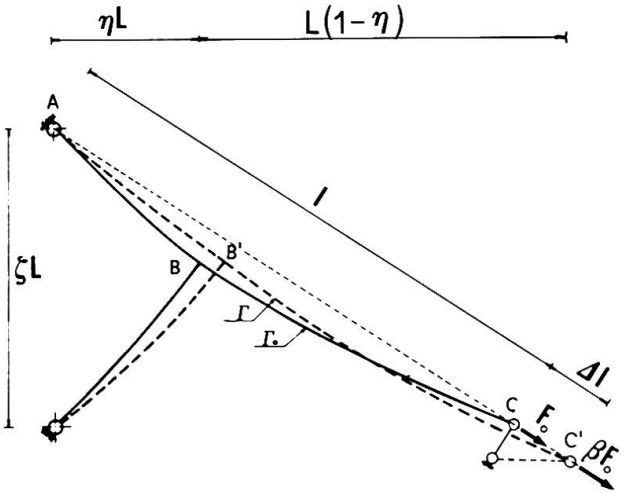

Fig. 8. Counter-stayed stay scheme: notation.

Obviously, a more accurate study for the nonlinear behaviour of this scheme must account for the influence of the ratio $n = \sigma_0/\sigma_0'$ of the initial stress σ_0 in the main stay versus that of the counter-stay, σ_0', and of the ratio $n' = A'/A$ between the counter-stay's area A' and that of the stay, A.
The analysis was made by using the second F.E. model.
In figs. 9.a, b the ratio E_s^*/E_{sd}^* is plotted as a function of the counter-stay's position parameter η. The secant modulus E_s^* is given by Eq. 19 for the simplified model and by Eq. 18 for the F.E. nonlinear model. E_{sd}^* is the secant modulus of the single main stay.
Figs. 9.a, b, are drawn for two different values of the β parameter, and also show the influence of the main stay's slope parameter ς. We observe first that:

i) a consistent loss of the ratio E_s^*/E_{sd}^* is shown by the nonlinear analysis in comparison with the simplified model,
ii) the optimum counter-staying position depends on the slope of the main stay.

This fact, which does not appear from the simplified model, is caused by the non-uniform stress distribution along the stay.

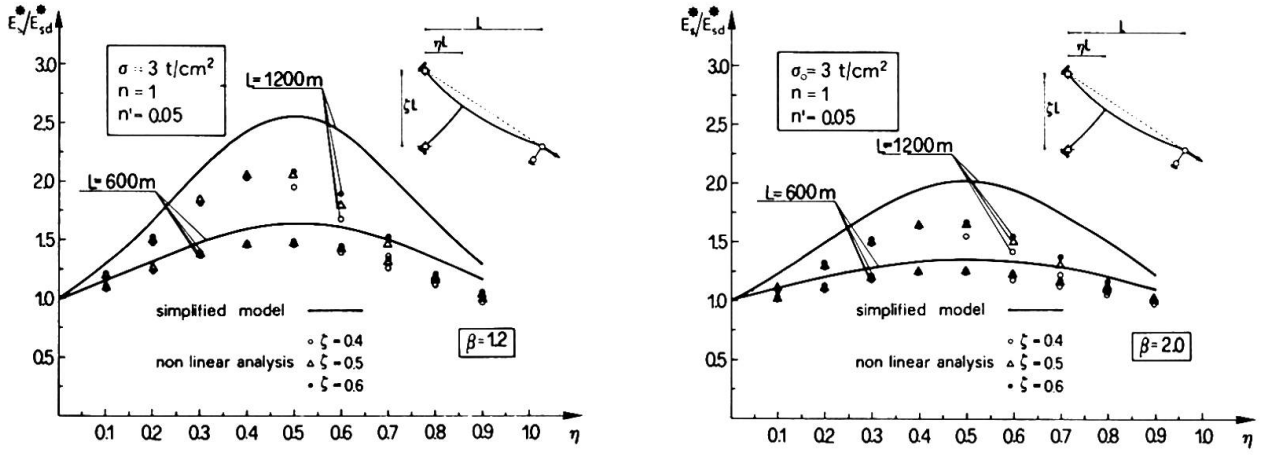

Fig. 9. Counter-stayed stay elastic response: influence of ς.

Further, we observe that the increase of axial stiffness, for a given ς, depends on the values of β parameter and that it is higher when β is close to 1 (fig. 10).

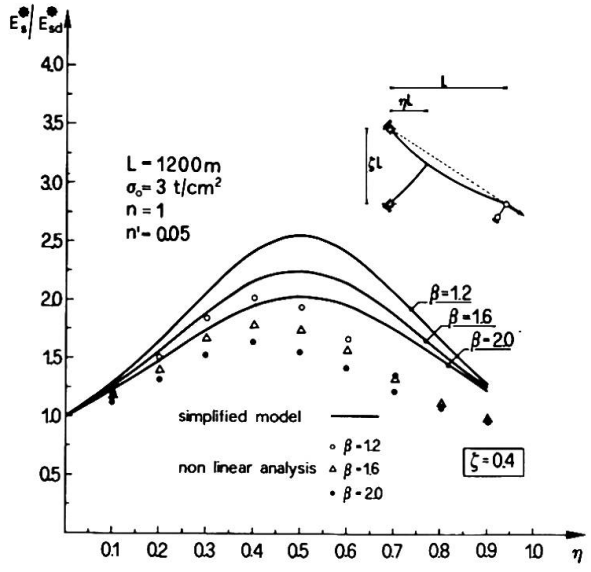

Fig. 10. Counter-stayed stay elastic response: influence of β.

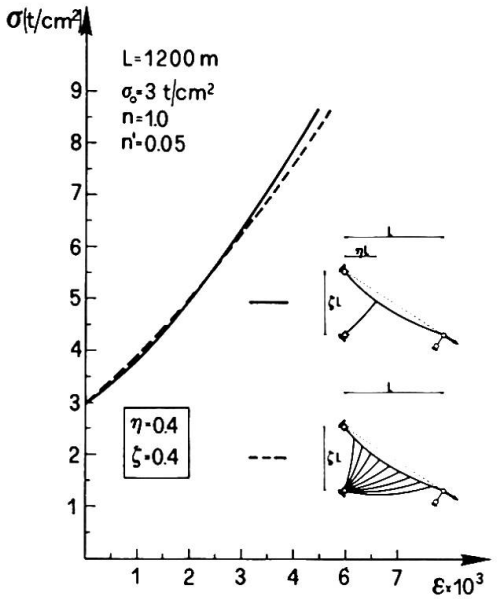

Fig. 11. Counter-stayed stay elastic response: influence of counter-stays' number.

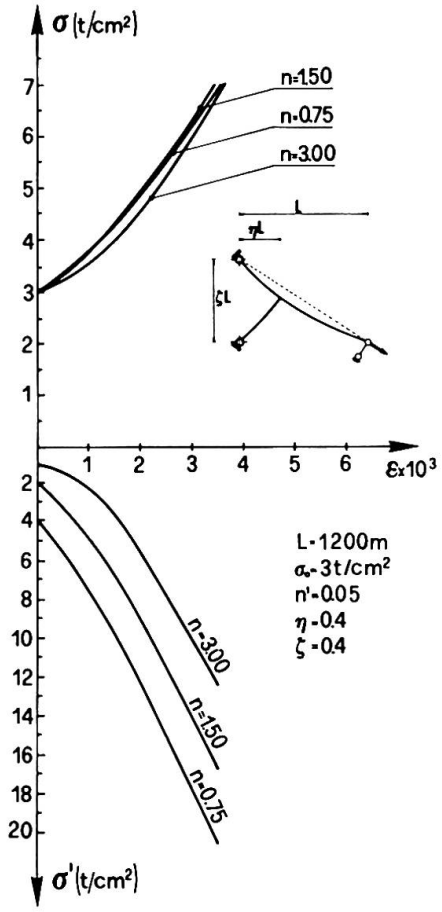

Fig. 12. Counter-stayed stay elastic response: influence of n.

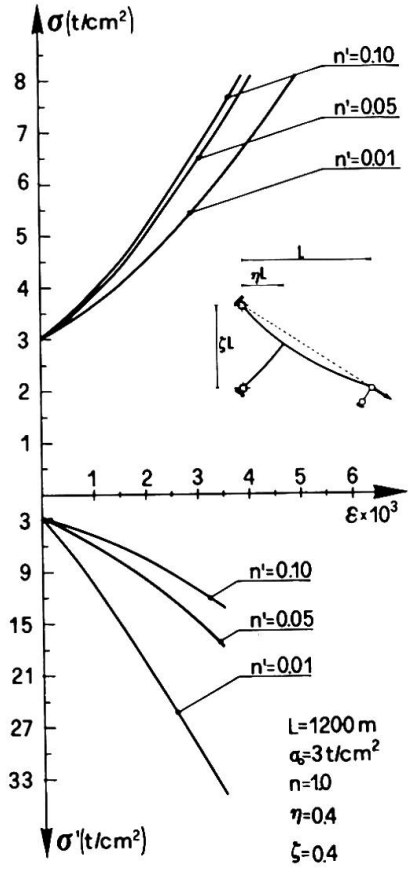

Fig. 13. Counter-stayed stay elastic response: influence of n'.

In fig. 11 the elastic response of a main stay with a diffused counter-stay system is compared with

that of a single counter-stayed main stay. The comparison is made for equivalent area of the two counter-stay systems. The elastic responses are practically equivalent: for this reason, the use of a single counter-stay in optimum position can be considered as definitely better.
In figs. 12, 13, the influence of $n = \sigma_0/\sigma'_0$ and of $n' = A'/A$ respectively is shown on the main stay's stiffening effect and on the stress level σ' in the counter-stay.
It may be observed that:

i) the main stay's stiffness increases as n decreases. But, the increase's improvement is practically uninfluenced for n smaller than a limiting value (in fig. 12, $n \simeq 1.5$). On the other hand, the stress σ' greatly increases as n decreases.
For this, we conclude that n cannot be reduced too much, for strength reasons.

ii) The axial stiffeness increase of the main stay is an increasing function of n'. But, the improvement reduces as n' increases. On the other hand, we observe that small values of n' induce unacceptable values of counterstayed stress level σ'.
It is therefore necessary to bound below the ratio n' (in fig. 13, $n' \geq 0.05$).

5. EXPERIMENTAL ANALYSIS.

An experimental analysis was carried out in order to permit the investigation of the correspondence of the elastic theories discussed in previous sections to the real behaviour of stayed systems.

5.1 The testing apparatus.

The schemes tested in our investigation are shown in fig. 14.

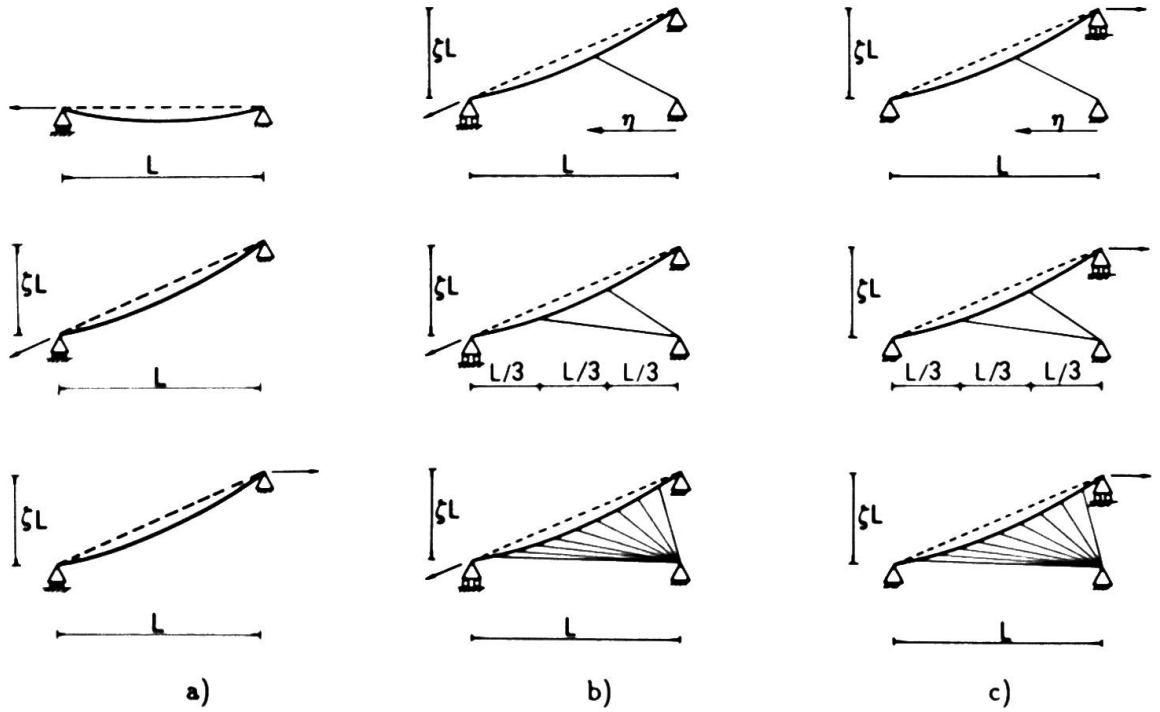

Fig. 14. Testing schemes.

Fig 14.a refers to the models of a single stay with horizontal or with inclined chord, while figs. 14.b, c refer to a system with counter-stays acting on a cable.
All the physical models, corresponding to these schemes, have been assembled on a steel frame (fig. 15.a, b). In all the cases examined, high elastic modulus steel stays have been used. The cable stress is measured at the fixed end by means of a HBM Mod. U2 load cell branched on a HBM Mod. MK measuring station.

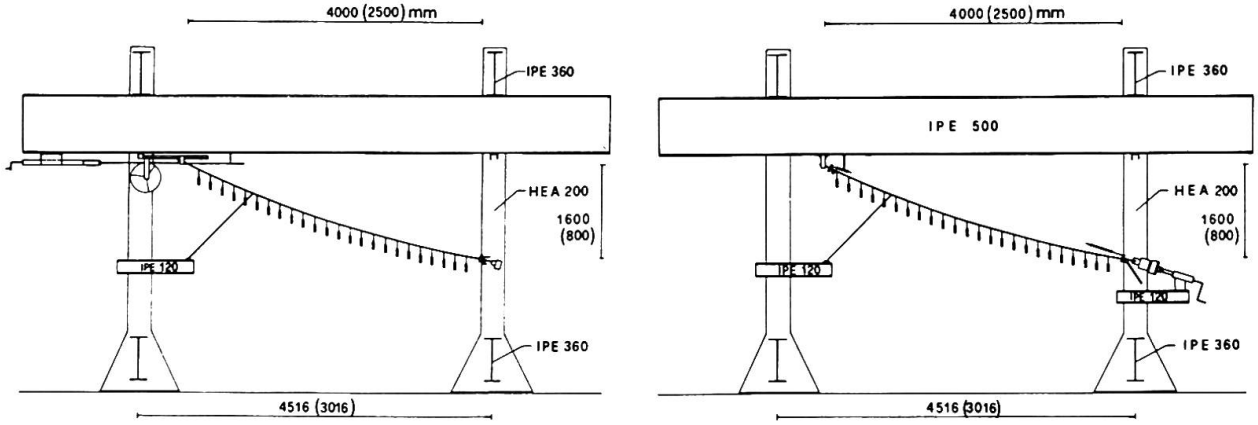

a) b)

Fig. 15. Testing apparatus.

Successively, for better accuracy, especially at low stress levels, a HBM Mod. Z3H2 load cell has been used.

This scheme allows to overcome the difficulty in determining the load loss due to friction at the moving end.

To obtain cable strains, displacements are measured by means of two couples of inductive displacement transducers applied at the fixed and moving ends, respectively.

To establish the mechanical similarity of the experimental model to a full scale stay, we assume the length and the specific force as fundamental quantities.

In our experiments the stress scale factor χ was assumed equal to unity, while the geometrical model parameter ς has been everywhere assumed $\varsigma = H_m/L_m = 0.32$.

As far as the model length L_m and the model cable diameter D_m are concerned, the following values have been used:

$$L_m = (2.50 \div 4.00m) \,, \quad D_m = (1.00 \div 1.80mm) \,.$$

The cable's Young modulus has been determined experimentally, and the obtained value is: $E = 2.0075 \times 10^7 \ t/m^2$.

The specific weight of the corresponding model has been simulated by means of an additional load p acting on the cable (figs. 14, 15).

5.2. Single stay experimental analysis.

We study the stay scheme shown in fig. 14.a), in relation to a single cable. The experimental investigation was carried out for two values of the characteristic parameter σ_0 ($\sigma_0 = 3 \div 4 \ \ t/m^2$), three values of L ($L = 350 \div 500 \div 900 \ \ m$) and many values of β. In fig. 16 some comparisons with the numerical results obtained via finite elements and via Dischinger's formula are given.

The elastic response curve $\sigma - \epsilon$ displays good agreement between the numerical results and the experimental ones at high stress level for the case of an inclined chord. On the other hand, at low stress levels, the numerical results obtained via finite elements and the experimental ones still agree, while significant differences from Dischinger's results can be observed.

Furthermore, the numerical and experimental results have been processed to give more effective information about the main characteristics of the elastic response, that is the secant modulus of the stay. In figs. 17.a,b, the difference between numerical results and experimental ones with respect to secant modulus, versus the stress level σ is shown. In particular, from fig. 17.a we observe a remarkable discrepancy (35%) between Dischinger's results and both those obtained via finite elemets and experimentally at low stress levels. Instead, from fig. 17.b we observe that the maximum percentage gap between the finite element results and the experimental ones is about 6%.

Finally, the experimental results have been used to determine the least square curve:

$$\delta = f(\alpha) \ , \tag{22}$$

where

$$\delta = E/E_s^* \ , \ \alpha = \frac{\gamma^2 L^2 E}{12\sigma_0^3} \frac{1+\beta}{2\beta^2} \ . \tag{23}$$

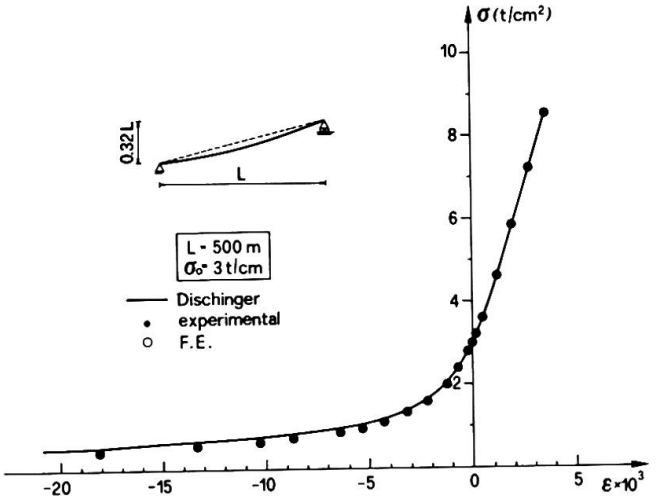

Fig. 16. Elastic response curve $\sigma - \epsilon$: comparison between theory and experiments.

Obviously, if we employ Dischinger's formula 11, Eq. 21 becomes:

$$\delta = 1 + \alpha \ . \tag{24}$$

Therefore, the experimental results have been used to determine the coefficients a, b of the regression line defined as:

$$\delta = a + b\alpha \ . \tag{25}$$

The computation was made using 92 experimental points [10] relative to cables with an inclined chord. We obtained:

$$a = 1.153 \ , \quad b = 0.691 \ . \tag{26}$$

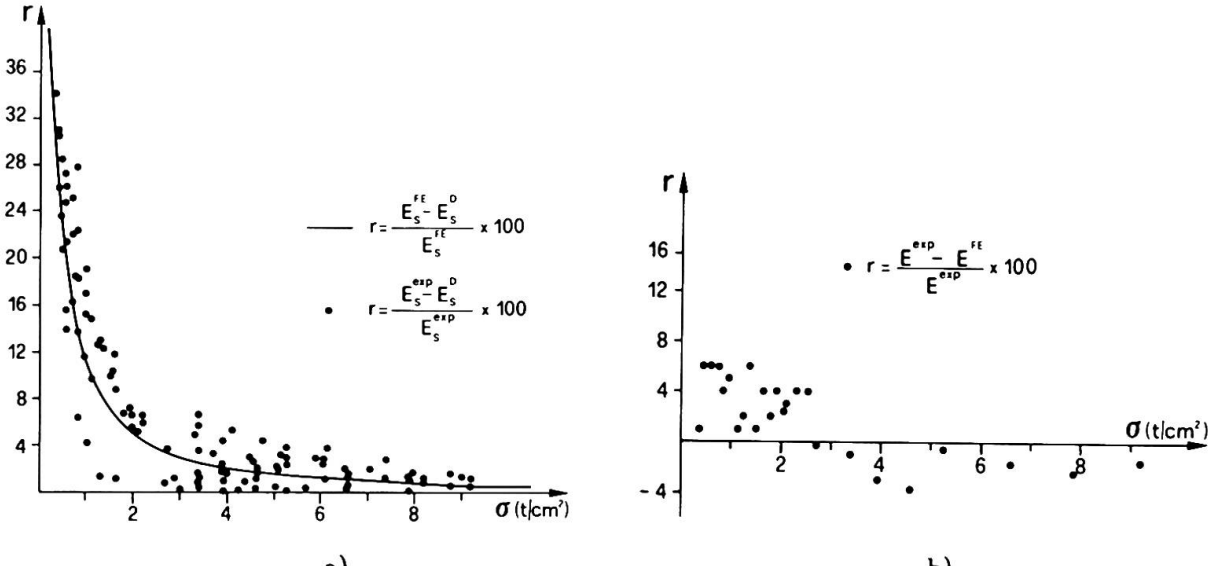

Fig. 17. Difference between theoretical and experimental values of the secant modulus versus stress levels.

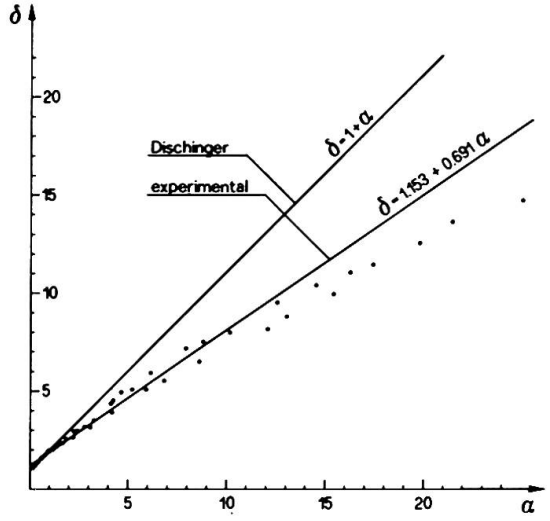

Fig. 18. Linear regression on $\alpha - \delta$ data.

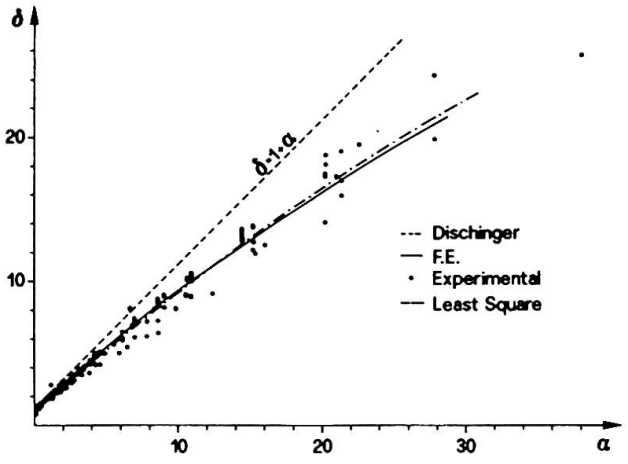

Fig. 19. Quadratic regression on $\alpha - \delta$ data.

On the other hand, if we use only 64 points referring to the stress level $\sigma \geq 3 \quad t/cm^2$ to determine the coefficients a, b, we get:

$$a = 0.998 \quad , \quad b = 0.990 \quad . \tag{27}$$

Therefore, it appears that the discrepancies shown (fig. 18) by the graphs corresponding to Eqs. 23 and 25 must be attributed to the inadequacy of Dischinger's theory at low stress levels, and this is also apparent from tab. 2.

In fig. 19, a further comparison is done among Dischinger's line (Eq. 24), experimental results, finite element results and the curve:

$$\delta = a + b\alpha + c\alpha^2 \quad , \tag{28}$$

where coefficients a, b, c were determined with the least square method, taking into account all the experimental points.

However, the accuracy of the experimental investigation is measured by the correlation factor r, whose values are given in tab. 2.

Table 2

$\sigma \geq$ (t/cm^2)	N. of experimental points	a	b	r
0	92	1.153	0.691	0.993
1	69	1.032	0.874	0.992
2	54	1.007	0.947	0.993
3	46	0.998	0.990	0.998

5.3. Counter-stay systems analysis.

In this section we analyze the behaviour of the counter-stayed stays, as shown in figs. 14.b, c. Firstly, we study the simple scheme of a single counter-stay acting on a cable. As pointed out in previous section 4, approximate analysis of this scheme can be made under Dischinger's assumption by using Eq. 21 while a more accurate numerical analysis can be carried out via finite elements by taking into account the actual elastic characteristic of the counter-stay element.

The comparison between theoretical and experimental results will be made with reference to the two schemes shown in fig. 20.

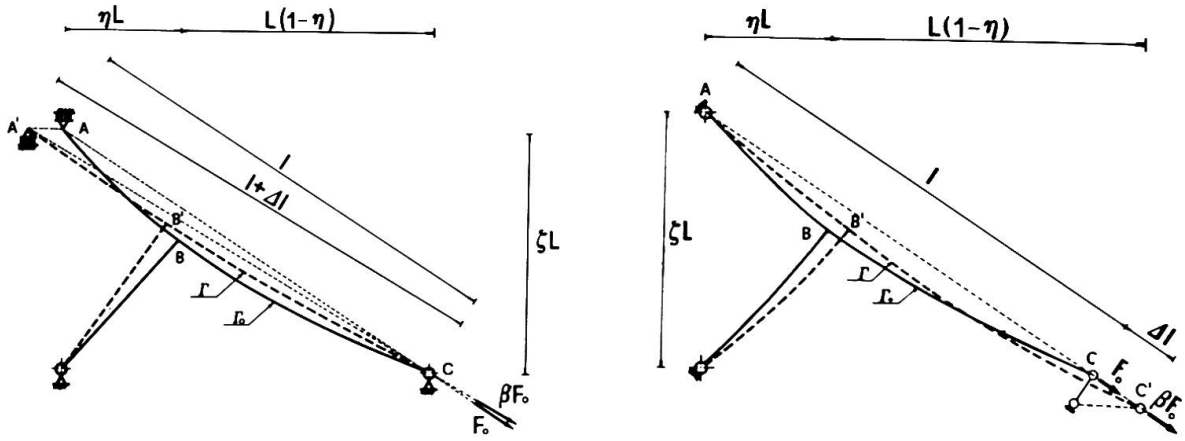

a) b)

Fig. 20. Schemes of counter-stayed systems.

These schemes correspond to a displacement imposed at end A or B of the main stay respectively. According to Dischinger's theory, the elastic response of the two schemes is the same. But, both nonlinear F.E. theory and, as we will show later, experiments, exhibit different behaviour.
As a matter of fact, in fig. 21 results are shown referring to single counter-stayed stay; we point out that the optimum staying position resulting both from F.E. and experiments is quite different from that based on Dischinger's theory.

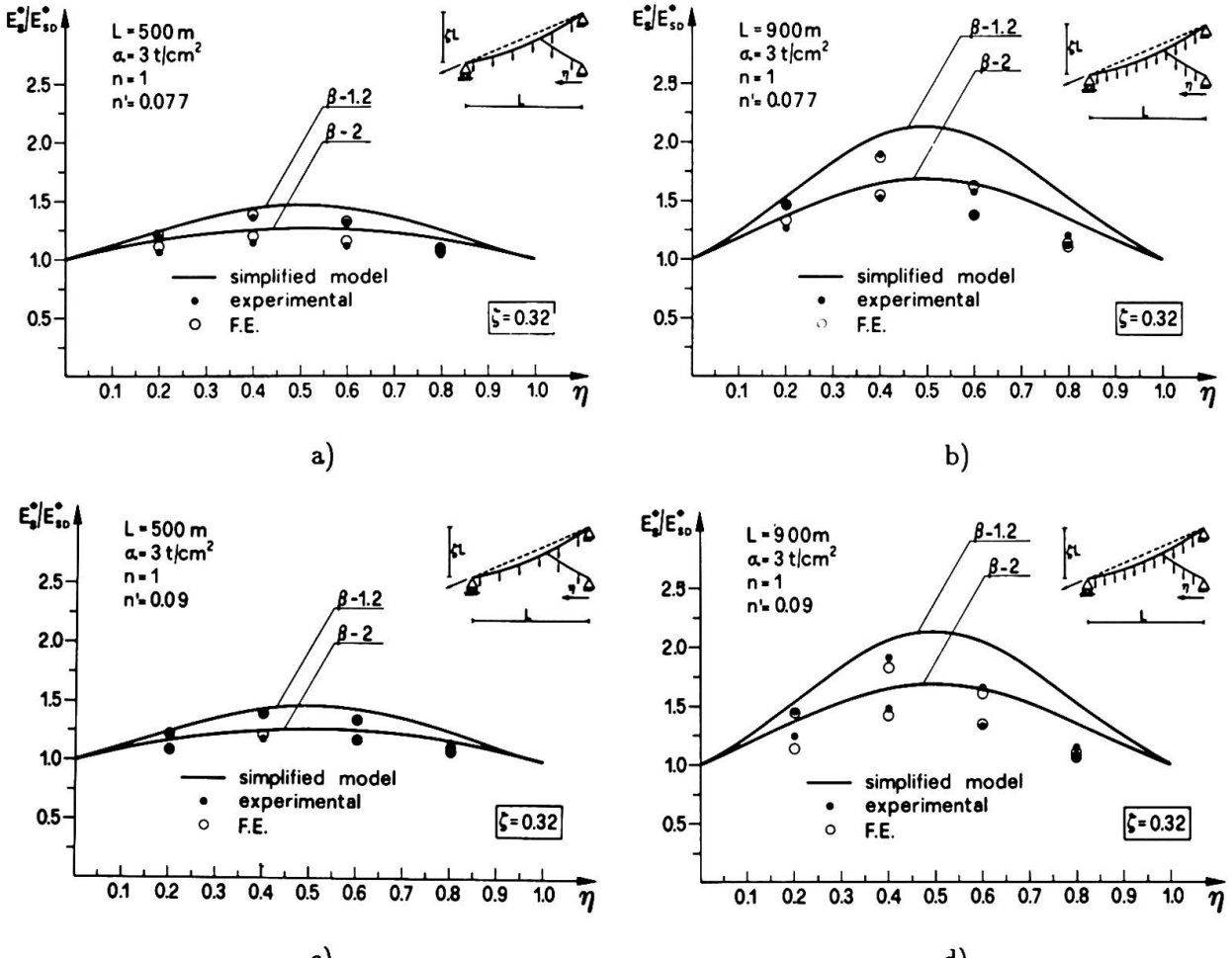

Fig. 21. Counter-stayed stay elastic response for different L, n' values.

Moreover, the counter-stay stiffening effect is overestimated if Dischinger's simplified theory is used.

In fig. 22 we compare the single counter-stay scheme under load conditions described in fig. 20. We observe a rather different elastic response, increasingly so as L increases. Experiments and F.E. computations agree very well and both grasp this essential feature of the structural behaviour. We point out that the scheme of fig. 20.b is more stiff.

Finally, we considered, from an experimental point of view, the influence of the number of counter-stays N_c. For the last condition depicted in fig. 20.b, we experimentally determined the ratio E_s^*/E_{sd}^* for different values of N_c and a constant total weight of the counter-stays.

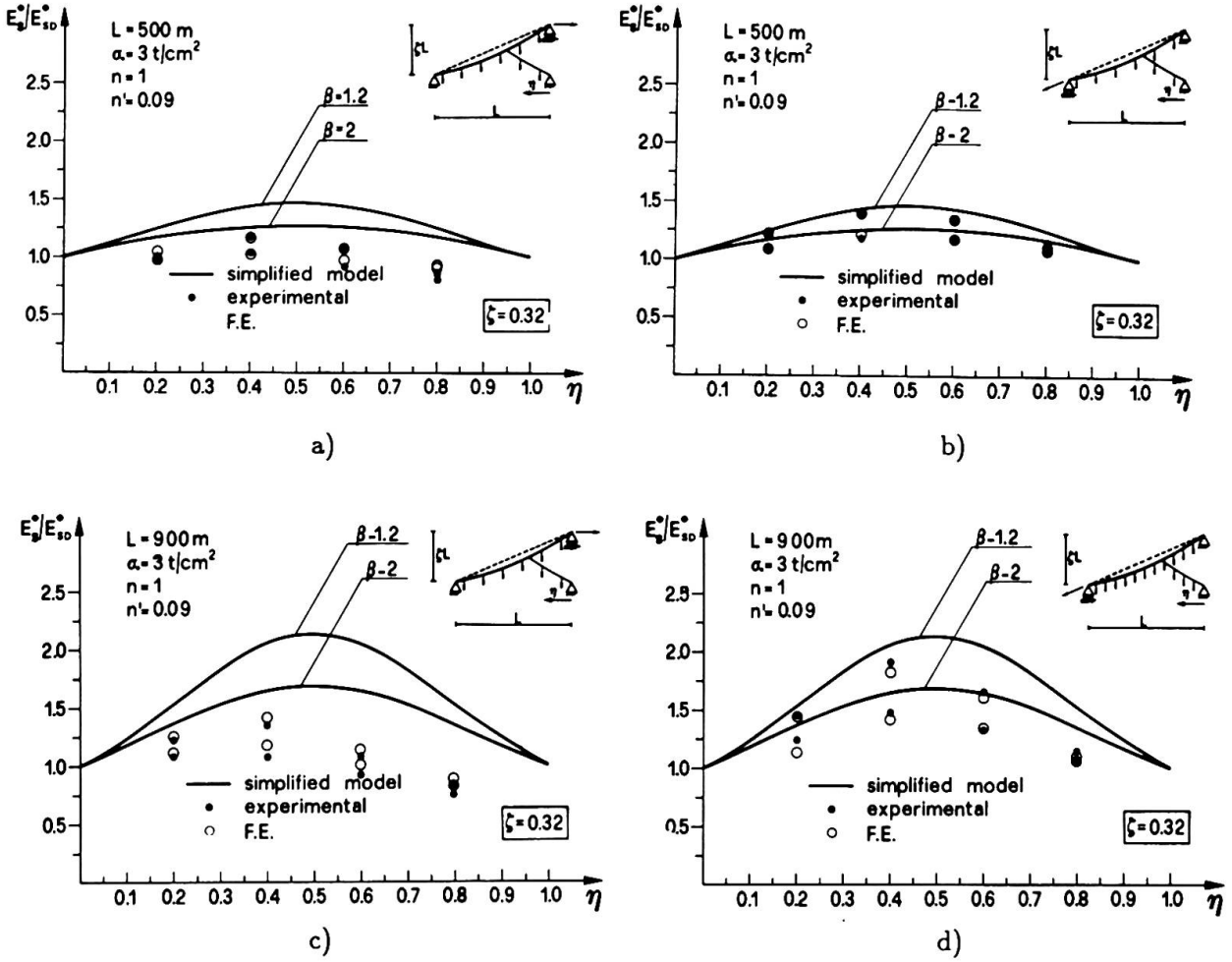

Fig. 22. Counter-stayed stay elastic response to a given end displacement for different L values.

In tab. 3, results obtained for $L = 500$ m and $L = 900$ m are shown. We point out that, in good agreement with the F.E. theory, the stiffening effect of the counter-staying system is almost independent of N_c. A single stay in optimum position therefore would be more suitable.

Table 3

	L = 500						L = 900					
	$N_c = 1$, $\eta = 0.4$		$N_c = 2$		$N_c = 9$		$N_c = 1$, $\eta = 0.4$		$N_c = 2$		$N_c = 9$	
β	E^*_{sp}/E^*_{SD}	E^*_{EF}/E^*_{SD}	E^*_{sp}/E^*_{SD}	E^*_{EF}/E^*_{SD}	E^*_{sp}/E^*_{SD}	E^*_{EF}/E^*_{SD}	E^*_{sp}/E^*_{SD}	E^*_{EF}/E^*_{SD}	E^*_{sp}/E^*_{SD}	E^*_{EF}/E^*_{SD}	E^*_{sp}/E^*_{SD}	E^*_{EF}/E^*_{SD}
1.2	1.383	1.391	1.406	1.424	1.408	1.422	1.737	1.820	1.884	1.854	1.834	1.892
2.0	1.165	1.206	1.173	1.215	1.159	1.210	1.452	1.451	1.451	1.478	1.413	1.473

6. CONCLUSIONS.

In this paper we studied some features of cables and cabled systems under their own weight and axial thrust, characteristic of structural elements employed as a part of a cable-stayed bridge.
As a matter of fact, the nonlinear stress–strain constitutive relationship of a stay is of central importance in the analysis of bridge deformability problems.
In particular, side span load can induce stays unloading, and in this case a refined nonlinear theory is needed to grasp the real structural behaviour.
Therefore, under the realistic hypothesis of a linear elastic material, we developed nonlinear finite element models appropriate to the analysis of stay's unloading or of complex schemes such as counter-stayed systems.
A wide numerical investigation was developed and the real behaviour of stays at low stress levels was shown to exist.
Finally, an experimental analysis was carried out, showing a very good agreement between our non-linear finite elements theories and tests.
In conclusion, the discrete model based on the proposed finite element schemes seems to be a viable instrument to give a sound simulation of the mechanical behaviour of the examined cable-based structural elements.

ACKNOWLEDGEMENTS.

This work was granted by the National Research Council (CNR) of Italy, at the "Nucleo di Studio sulle Grandi Strutture", University of Rome 2.

REFERENCES.

[1] Irvine H.M., Analytical Solutions for pretensioned cable nets. Journal of the Eng. Mechanics Division, EM1, 43-57, Feb. 1976.
[2] Hengold W.M. and Russel J.J., Equilibrium and natural frequencies of cable structures (a nonlinear finite element approach). Computer and Structures, Vol. 6, 267-271, 1976.
[3] Irvine H.M. and Sinclair G.B., The suspended elastic cable under the action of concentrated vertical loads. Int. J. Solids Structures, Vol. 12, 309, 1976.
[4] Troitsky M.S., Cable–stayed bridges. Crosby Lockwood Staples, London, 1977.
[5] Leonhardt F. and Zellner W., Cable–stayed bridges. IABSE Surveys S-13/80, May 1980.
[6] Rajaram A., Loganathau K. and Roman N.V., Nonlinear analysis of cable–stayed bridges. IABSE Proc., 37-80, Nov. 1980.
[7] Sinclair G.B. and Hodder S.B., Exact solutions for elastic cable systems. Int. J. Solids Structures, Vol. 17, 845-854, 1981.
[8] Wang C.Y. and Watson L.T., The elastic catenary. Int. J. Mech. Sci., Vol. 24, N. 6, 349-357, 1982.
[9] Maceri F. and Bruno D., Non linear models for cable–stayed bridges analysis. 1st European Simulation Congress ESC 83, Aachen, Sept. 1983, Proc. ed. by W. Ameling, IFB 71, 631-644, Springer–Verlag.
[10] Bruno D., Maceri F. and Olivito R.S., An experimental study on the nonlinear behaviour of stays. XII Convegno AIAS, Sept. 24-27, Sorrento, 1984.
[11] Como M., Grimaldi A. and Maceri F., Statical behaviour of long–span cable–stayed bridges. Int. J. Solids Structures, Vol. 21, N. 8, 831-850,1985.
[12] Bruno D., Maceri F. and Olivito R.S., Stralli controventati: un'indagine sperimentale. XIV Convegno AIAS, Sept. 23-27, Catania, 1986.
[13] Bruno D., Maceri F. and Olivito R.S., An experimental analysis on the behaviour of stays and stayed system. The 4th National Symposium for Experimental Stress Analysis and Material Testing, Brasov – Romania, Sept. 24- 27, 1986.
[14] Bruno D. and Grimaldi A., Nonlinear behaviour of long–span cable–stayed bridges. Meccanica, 20 (1985), 303-313.